Original Article | Musculoskeletal Imaging

http://dx.doi.org/10.3348/kjr.2014.15.1.114
pISSN 1229-6929 · eISSN 2005-8330
Korean J Radiol 2014;15(1):114-122

Korean Journal of Radiology
KJR

MR Findings of the Osteofibrous Dysplasia

Joon-Yong Jung, MD[1], Won-Hee Jee, MD[1], Sung Hwan Hong, MD[2], Heung Sik Kang, MD[3], Hye Won Chung, MD[4], Kyung-Nam Ryu, MD[5], Jee-Young Kim, MD[1], Soo-A Im, MD[1], Jeong-Mi Park, MD[1], Mi-Sook Sung, MD[1], Yeon-Soo Lee, MD[1], Suk-Joo Hong, MD[6], Chan-Kwon Jung, MD[7], Yang-Guk Chung, MD[8]

Departments of [1]Radiology, [7]Pathology, and [8]Orthopedic Surgery, College of Medicine, The Catholic University of Korea, Seoul 137-701, Korea; [2]Department of Radiology, Seoul National University College of Medicine, Seoul 110-744, Korea; [3]Department of Radiology, Seoul National University Bundang Hospital, Seongnam 463-707, Korea; [4]Department of Radiology, Asan Medical Center, University of Ulsan College of Medicine, Seoul 138-736, Korea; [5]Department of Radiology, Kyung Hee University College of Medicine, Seoul 130-872, Korea; [6]Department of Radiology, Korea University College of Medicine, Seoul 136-705, Korea

Objective: The aim of this study was to describe MR findings of osteofibrous dysplasia.

Materials and Methods: MR images of 24 pathologically proven osteofibrous dysplasia cases were retrospectively analyzed for a signal intensity of the lesion, presence of intralesional fat signal, internal hypointense band, multilocular appearance, cortical expansion, intramedullary extension, cystic area, cortical breakage and extraosseous extension, abnormal signal from the adjacent bone marrow and soft tissue and patterns of contrast enhancement.

Results: All cases of osteofibrous dysplasia exhibited intermediate signal intensity on T1-weighted images. On T2-weighted images, 20 and 4 cases exhibited heterogeneously intermediate and high signal intensity, respectively. Intralesional fat was identified in 12% of the cases. Internal low-signal bands and multilocular appearance were observed in 91%. Cortical expansion was present in 58%. Intramedullary extension was present in all cases, and an entire intramedullary replacement was observed in 33%. Cortical breakage (n = 3) and extraosseous mass formation (n = 1) were observed in cases with pathologic fractures only. A cystic area was observed in one case. Among 21 cases without a pathologic fracture, abnormal signal intensity in the surrounding bone marrow and adjacent soft tissue was observed in 43% and 48%, respectively. All cases exhibited diffuse contrast enhancement.

Conclusion: Osteofibrous dysplasia exhibited diverse imaging features ranging from lesions confined to the cortex to more aggressive lesions with complete intramedullary involvement or perilesional marrow edema.

Index terms: *Osteofibrous dysplasia; Bone neoplasms; Magnetic resonance imaging*

Received May 13, 2013; accepted after revision September 7, 2013.
Corresponding author: Won-Hee Jee, MD, Department of Radiology, Seoul St. Mary's Hospital, College of Medicine, The Catholic University of Korea, 222 Banpo-daero, Seocho-gu, Seoul 137-701, Korea.
• Tel: (822) 2258-6238 • Fax: (822) 599-6771
• E-mail: whjee@catholic.ac.kr

INTRODUCTION

Osteofibrous dysplasia, also termed ossifying fibroma of long bones, is a rare benign fibro-osseous lesion that has a strong predilection for an involvement of the tibia in the early childhood. The biologic behavior of osteofibrous dysplasia is reportedly diverse, ranging from non-progressive to recurrent and more aggressive lesions. Regardless of the wide spectrum of growing tendencies, most of the lesions become quiescent or even regress spontaneously as skeletal

Korean Journal of Radiology
KJR

maturation is completed (1-4).

Typical radiographic findings of osteofibrous dysplasia reveal eccentric, fairly well-marginated osteolytic lesions with a sclerotic border in the anterior cortex of the tibial diaphysis. As the lesion progresses, it exhibits a longitudinal spread to metaphysis, cortical expansion, intramedullary extension and anterior bowing deformity (5, 6). While radiographic findings of osteofibrous dysplasia are well-established, magnetic resonance (MR) imaging findings of osteofibrous dysplasia have not been fully described in the literature and have been reported anecdotally only (7-9). The purpose of the present study was to describe MR imaging findings of osteofibrous dysplasia.

MATERIALS AND METHODS

The study protocol was approved by the institutional review board, and the requirement for a written informed consent was waived. The study complied with the Health Insurance Portability and Accountability Act guidelines. The patient records between May 1994 to September 2012 were searched for all patients with a pathologically proven diagnosis of "ossifying fibroma" or "osteofibrous dysplasia" from the databases of nine different institutions. Pathologic diagnoses of ossifying fibroma were based on the commonly accepted histologic criteria (9, 10). A diagnosis of osteofibrous dysplasia was made when trabeculae of woven bone lined by osteoblasts appeared within a fibrous stroma, where the nests of epithelial cell could not be identified on routine hematoxylin and eosin staining. A total of 31 patients were found from the databases. Among them, three patients with ossifying fibromas in the mandible or maxilla were excluded, as the ossifying fibroma of the jaw is regarded a different disease entity from ossifying fibroma in the long bone. Four patients whose MR images were not available in the image analysis due to the absence or poor image quality were also excluded. Finally, 24 patients (16 male and 8 female; age range, 2-42 years; mean age, 15 years) were included in this study.

Magnetic resonance images were retrospectively analyzed by a consensus of two reviewers regarding the following characteristics: a predominant signal intensity of the lesion on T1-weighted and T2-weighted images, a presence of intralesional fat signal, an internal hypointense band, multilocular appearance, a cystic area, cortical expansion, intramedullary extension, an abnormal adjacent bone marrow and soft tissue signal and patterns of contrast enhancement. The signal intensity of lesions was classified relative to those of muscles and fat on T1-weighted images (11): low when the signal intensity was less than that of muscle; intermediate when the signal intensity was similar to that of muscle; and high when the signal intensity was greater than that of muscle and approaching that of fat. Similarly, the signal intensity of lesions on T2-weighted images were also classified relative to those of muscles and fat (11): low when the signal intensity was similar to that of muscle; intermediate when the signal intensity was similar to that of fat; and high when the signal intensity was greater than that of fat. Definition of the signal intensity of lesions was modified on T2-weighted images obtained with fast spin-echo or fat-suppression: low when the signal intensity was similar to that of muscle; intermediate when the signal intensity was greater than that of muscle but far less than that of fat or fluid; and high when the signal intensity was far greater than that of muscle and approaching to that of fat or fluid. Cortical expansion was defined as the thickness of the bony cortex adjacent to the lesion, being obviously wider than the expected thickness at the region. Intramedullary extension was defined as a replacement of medullary cavity by the lesion, and if present, further graded either partial or complete intramedullary extension. An abnormal signal of bone marrow or adjacent soft tissue, which likely indicated perilesional edema or infiltration, was graded by the overall width of the signal: mild (< 1 cm); moderate (1-2 cm); or severe (> 2 cm). A presence of intralesional fat was recognized by a high signal intensity portion on both T1-weighted and T2-weighted images, and which was suppressed on fat suppression sequences. The enhancement pattern was divided into homogeneous or heterogeneous. Heterogeneously enhanced cases were classified further into one of the following patterns: diffuse, peripheral, central or marginal septal enhancement.

Magnetic resonance imaging was performed using various 1.0T or 1.5T systems with a general-purpose surface coil or body coil. In all cases, T1-weighted MR images (repetition time msec/echo time msec = 350-650/11-30) and conventional spin-echo T2-weighted (1800-2700/60-100) or fast spin-echo T2-weighted (2500-4000/76-108) images with or without fat-suppression were obtained. In all cases, longitudinal and axial fat-suppressed T1-weighted imaging was performed after an infusion of 0.1 mmol/kg of body weight of gadopentetate dimeglumine (Magnevist; Schering, Berlin, Germany). Typical MR imaging parameters

were as follows: field of view, 10-30 cm; matrix size, 256 x 192; section thickness, 3-8 mm; intersection gap, 1.5-2.0 mm; and echo-train length, four to eight.

RESULTS

Radiologic findings are summarized in Table 1. In all cases, osteofibrous dysplasia was composed mainly of intracortical lesions and exhibited intramedullary extension in variable degrees. Of the 24 lesions, 22 involved the tibia and the remaining two involved the fibula. All lesions were mainly located in the diaphysis with a propensity for the proximal diaphysis and extension to the proximal metaphysis. Nearly all cases exhibited anterior cortical involvement, with the exception of one case with posterior cortical involvement. Bowing deformity was observed in 58% (14/24) of the cases. Multiplicity was observed in four cases. Of these, three had a satellite lesion separated from the main lesion by an intervening normal bone in the same bone, whereas one case had bilateral tibial involvement. Pathologic fracture occurred in three cases.

On T1-weighted images, all lesions exhibited an intermediate signal intensity similar to that of muscle, with homogeneous (50%, 12/24) or heterogeneous (50%, 12/24) patterns (Figs. 1, 2). On T2-weighted MR images, 83% (20/24) of all cases exhibited an intermediate signal intensity. The remaining four cases exhibited a hyperintense signal intensity which was definitely higher than that of fat on T2-weighted images. Of the 24 cases, 20 exhibited heterogeneous signal intensity, and the remaining four exhibited homogeneous signal intensity on T2-weighted images. All lesions were surrounded by a peripheral low signal rim with variable thickness. Intralesional fat was identified in 12% (3/24) of all cases (Fig. 3). Plain radiography revealed that four cases involved a unilocular lesion without internal septa, while the remaining 20 cases were multilocular lesions. MR images revealed an additional two cases with septa among the four cases with unilocular appearance on plain radiography. Cortical expansion was observed in 58% (14/24) of the cases. Intramedullary extension was present in all cases, and complete intramedullary replacement was observed in 33% (8/24) of lesions. Cortical breakage and extraosseous mass formation were observed in three and one case, respectively. All cases with cortical breakage or extraosseous mass formation were associated with pathologic fractures. All cases with pathologic fracture exhibited moderate to severe degrees of abnormal signal intensity in the surrounding bone marrow and adjacent soft tissue (Fig. 2). Among 21 cases without pathologic fractures, abnormal signal intensity in the surrounding bone marrow and adjacent soft tissue was observed in 43% (9/21) and 48% (10/21) of the cases, respectively. Regarding the severity of the abnormal signal, five cases demonstrated mild degrees of abnormal signal intensity in the bone marrow, whereas remaining four exhibited moderate (2/21) or severe (2/21) degree of abnormal bone marrow signals. All cases without pathologic fracture demonstrated only a mild degree of abnormal signal intensity in the adjacent soft tissue. Contrast-enhanced images revealed that all cases exhibited intense

Table 1. Imaging Features of Osteofibrous Dysplasia

Imaging Finding	Radiography (n = 24)	MR Imaging (n = 24)
Bowing deformity	14 (58)	NA
Multiplicity	3 (13)	4 (17)
Internal septa/multilocular appearance	20 (83)	22 (92)
Pathologic fracture	2 (8)	3 (12)
Cortical expansion	14 (58)	14 (58)
Signal intensity on T1WI	NA	Intermediate in 24 (100) Heterogeneous vs. homogeneous: 12 (50) vs. 12 (50)
Signal intensity on T2WI	NA	Intermediate vs. hyperintense: 20 (83) vs. 4 (17) Heterogeneous vs. homogeneous: 20 (83) vs. 4 (17)
Enhancement pattern	NA	Diffuse in 24 (100) Heterogeneous vs. homogeneous: 16 (67) vs. 8 (33)
Intralesional fat content	NA	3 (38)
Perilesional bone marrow edema	NA	12 (50)
Soft tissue edema	NA	13 (54)

Note.— Data are numbers of patients, and numbers in parentheses are percentages. NA = not applicable, T1WI = T1-weighted image, T2WI = T2-weighted image

Korean Journal of Radiology
KJR

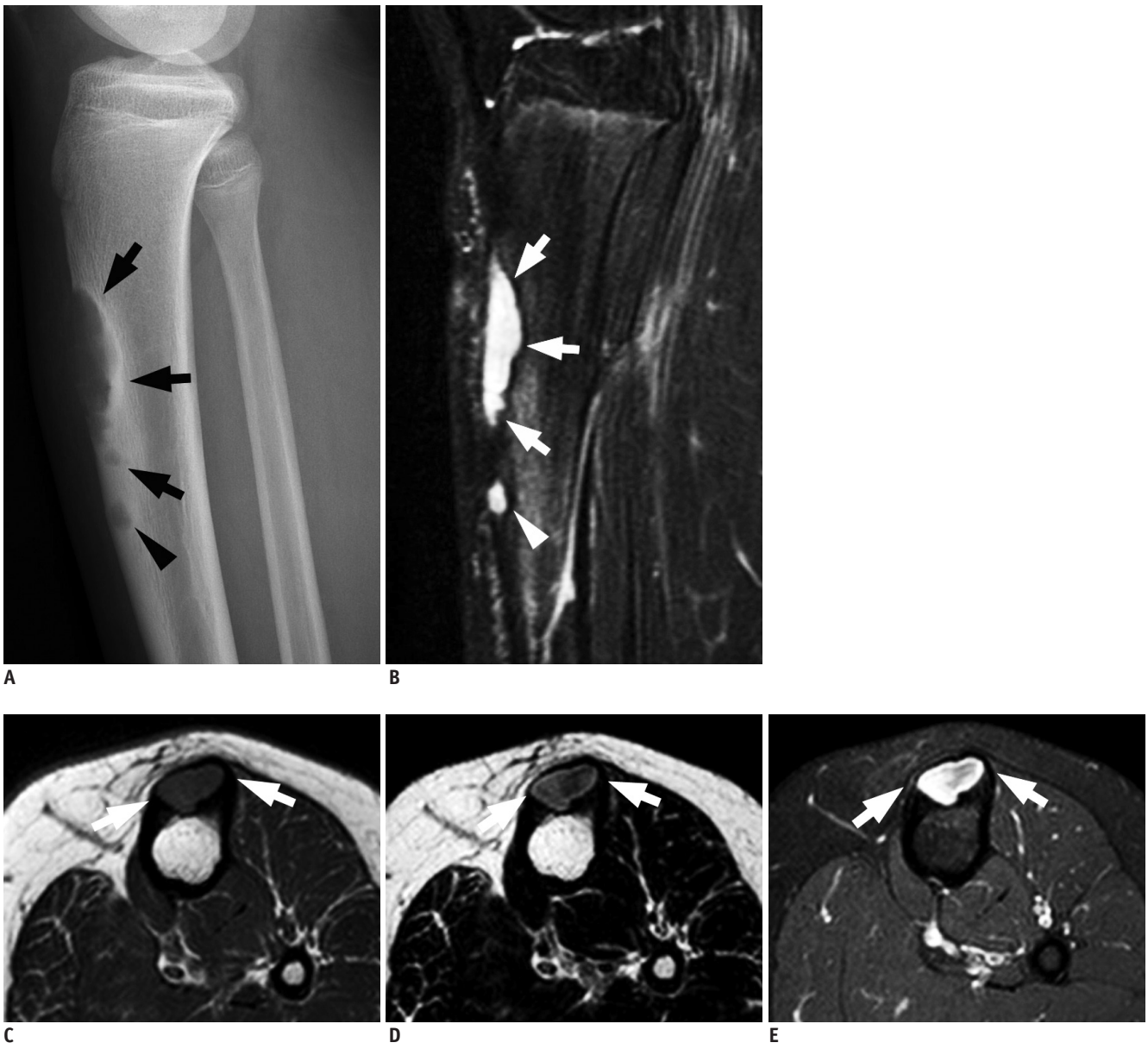

Fig. 1. 14-year-old boy presented with incidental radiographic abnormality during evaluation of left tibial pain after contusion.
A. Lateral radiograph shows well-defined osteolytic lesion (arrows) with thin sclerotic rim and internal septation in anterior cortex of proximal diaphysis of tibia and another smaller satellite lesion (arrowhead) in more distal cortex. **B.** Sagittal fat-suppressed T2-weighted image also shows main lesion (arrows) and satellite lesions (arrowhead) involving anterior cortex. **C, D.** Axial T1- and T2-weighted images show that mass (arrows) is mainly intracortical and exhibits intermediate signal intensity. **E.** On contrast-enhanced T1-weighted image, mass (arrows) exhibits diffuse heterogeneous enhancement.

enhancement with heterogeneous patterns (67%, 16/24) or homogeneous patterns (33%, 8/24). The enhancement patterns of all cases with heterogeneous enhancement did not correspond to any predetermined patterns, including peripheral, central or marginal septal enhancement; therefore, the lesions were classified as having a diffuse enhanced pattern. In only one case, a cystic area was observed within the lesion.

DISCUSSION

Osteofibrous dysplasia, also referred to as ossifying fibroma of long bones, is a benign fibro-osseous lesion composed of fibrous tissue with woven bone formation. The lesions exclusively occur in the tibia and fibula, although a case with ulnar involvement has been reported (12). Once osteofibrous dysplasia was identified as a variant of fibrous dysplasia, however, it was established as a distinct

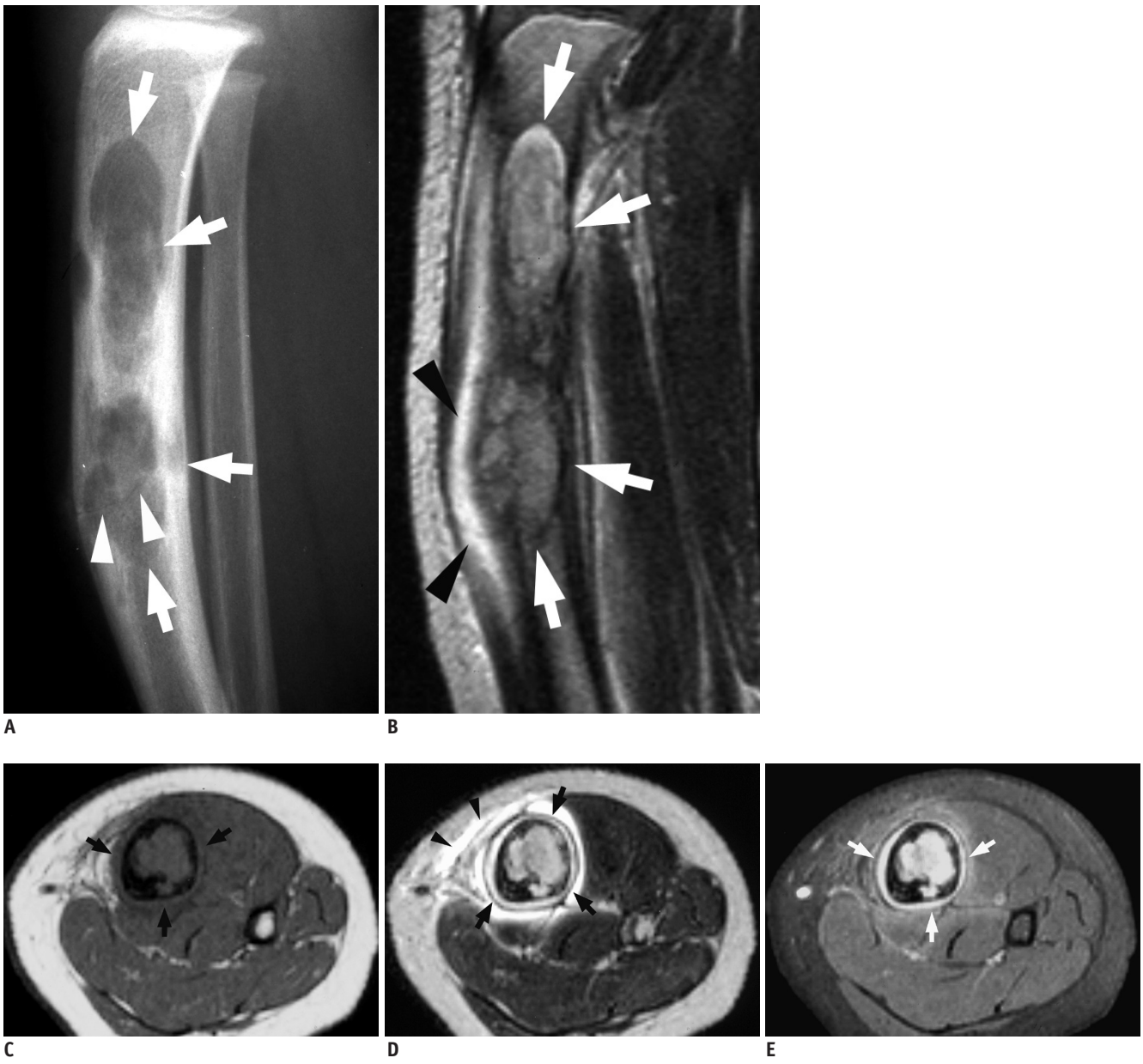

Fig. 2. 2-year-old boy presented with pain and pretibial swelling.
A. Lateral radiograph shows well-defined osteolytic lesion (arrows), with cortical expansion and anterior bowing. Fracture line is visible at mid-diaphysis (arrowheads). **B.** Sagittal T1-weighted image shows intermediate signal intensity mass (arrows) with soft tissue edema (arrowheads). **C, D.** Axial T1- and T2-weighted images show diffuse heterogeneous intermediate signal mass (arrows) replacing entire medullary space. Axial T2-weighted image also shows periosteal reaction with circumferential and pretibial soft tissue edema (arrowheads), presumably related to pathologic fracture. **E.** On axial contrast-enhanced T1-weighted image, mass exhibits diffuse heterogeneous enhancement with circumferential soft tissue enhancement (arrows).

lesion, because the characteristic zonal phenomenon and osteoblastic rimming of bony trabeculae were absent in fibrous dysplasia (5, 13). Although osteofibrous dysplasia and ossifying fibroma of the jaw share some histologic characteristics, the presence of cytokeratin-positive cells in the ossifying fibroma of the long bones and development of psammomatous calcification in the ossifying fibroma of the jaw are exclusive histopathologic features that distinguish the two as separate diseases (14, 15).

Radiographic findings of osteofibrous dysplasia have been well described in the literature (4-6, 8, 15). Osteofibrous dysplasia typically appears as an osteolytic lesion with lobular loculations to a bubbly appearance and circumscribed by a sclerotic border. It preferentially involves the anterior diaphyseal cortex of the tibia or fibula with adjacent cortical expansion. Intramedullary

Korean Journal of Radiology
KJR

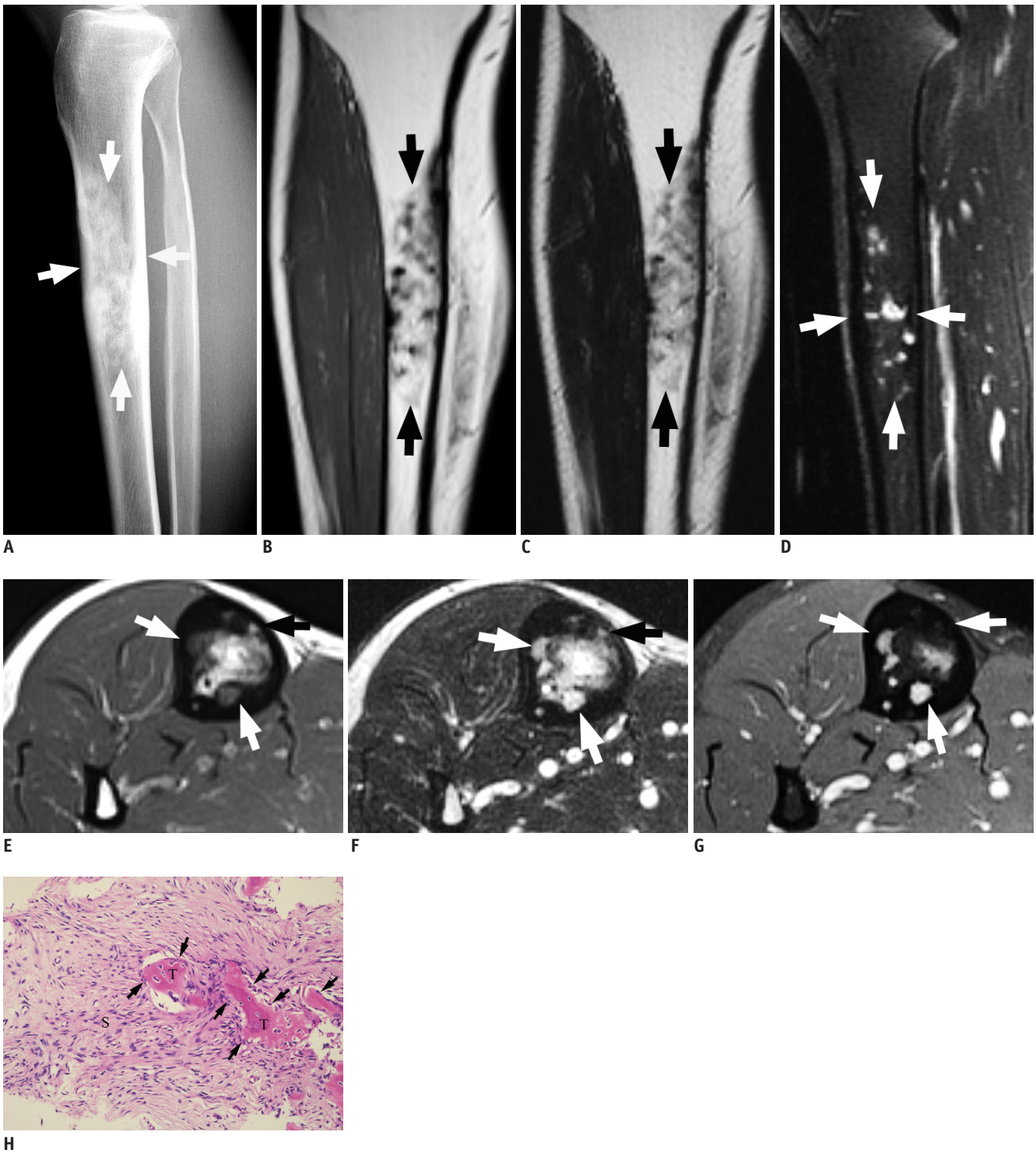

Fig. 3. 41-year-old woman presented with incidental radiographic abnormality in right tibia during evaluation of tingling sensation in right foot.

A. Lateral radiograph shows mix of bubbly osteolytic and sclerotic lesions (arrows) with indistinct borders on anterior tibial cortex. **B, C.** Coronal T1- and T2-weighted images show heterogeneously intermediate signal lesions (arrows) in diaphysis of right tibia. **D.** Sagittal fat-suppressed T2-weighted image shows lesion with multifocal nodular hyperintensities (arrows), corresponding to osteolytic foci in radiography. **E.** Axial T1-weighted image shows heterogeneously intermediate signal in lesion (arrows) replacing entire medullary cavity. **F.** Axial T2-weighted image also shows heterogeneously intermediate signals of lesion (arrows). **G.** On axial contrast-enhanced T1-weighted image, mass exhibits heterogeneous enhancement pattern with nodular enhancing foci (arrows). **H.** Irregular trabeculae (T) of immature bones have osteoblastic rimming (arrows) and are surrounded by fibrous stroma (S) without cytologic atypia (H&E stain, original magnification x 200).

encroachment and anterior bowing deformity are commonly associated as the lesion progresses. The MR findings of the osteofibrous dysplasia in our study were consistent with those of previously reported cases (7, 8, 16). The signal intensity of osteofibrous dysplasia was intermediate on T1-weighted images and intermediate to high on T2-weighted images. Cellularity, collagen density and degree of mineralization in osteoid matrix may attribute to the signal intensity. Superimposed hemorrhagic or cystic, myxoid change and even cartilaginous differentiation can modify the signal intensity and contribute to heterogeneous signal intensity on T2-weighted images (6, 17). However, osteofibrous dysplasia does not always show such patterns of signal intensity and are mostly similar to other tumors with fibroblastic stroma (18-20). No previous reports have focused on the contrast enhancement patterns of the ossifying fibroma of long bones. In this study, all cases exhibited diffuse and intense enhancement on the contrast-enhanced images. The relatively well-enhanced pattern is likely a reflection of rich fibrovascular stroma, similar to other fibrous tumors (19, 20).

Various researchers have suggested a relationship between ossifying fibroma of long bones and adamantinoma (8, 21-25). Adamantinoma is a rare low-grade malignant tumor that occurs primarily in the tibia. Besides its preferential involvement with the tibia, it shares radiologic and pathologic features with osteofibrous dysplasia. Although the older age distribution of adamantinoma and its more aggressive clinical behavior distinguish it from osteofibrous dysplasia, the diseases overlap considerably in clinical, radiological and histopathologic aspects (8, 26). Histologically, a detection of the nests or strands of epithelioid cell is the key to differentiating between adamantioma and osteofibrous dysplasia, although adamantinoma can contain variable amounts of osteofibrous dysplasia-like components (13, 23, 24). However, a certain type of adamantinoma has a scarce epithelioid component and is mostly composed of osteofibrous dysplasia-like tissue. This type of adamantinoma has been referred to as osteofibrous dysplasia-like adamantinoma, or juvenile adamantinoma, differentiated adamantinoma (27, 28). Many authors have hypothesized that osteofibrous dysplasia, osteofibrous dysplasia-like adamantinoma and adamantinoma may be different stages of the same disease that progresses from osteofibrous dysplasia to classic adamantinoma, based on observations of the histologic and immunohistochemical features (9, 28). However, contradictory evidences have also been reported and thus far, the relationship between osteofibrous dysplasia and adamantinoma is still controversial (6, 15, 25).

According to a previous report on MR findings of adamantinoma by Van der Woude et al. (21), the signal-intensity characteristics of osteofibrous dysplasia in our study are similar to those of adamantinoma. Given the fact that differentiated adamantinoma cases comprised a substantial proportion of their study compared with classic adamantinoma, the substantial similarity in the signal-intensity characteristics of adamantinoma in their study and osteofibrous dysplasia in the present study appears to be a corollary. However, they reported cortical breakage and soft tissue extension without pathologic fracture in 32% and 9% of adamantinoma cases, respectively. Meanwhile, cortical breakage and extraosseous extension to surrounding soft tissue were always associated with pathologic fractures in osteofibrous dysplasia in our study. Khanna et al. (8) suggested that a moth-eaten border and complete medullary involvement are potentially distinguishing radiological features of adamantinoma from osteofibrous dysplasia. However, those findings can also appear in osteofibrous dysplasia. In our study, complete medullary involvement was observed in 33% of osteofibrous dysplasia. Among them, there were two cases of which the initial diagnosis at the preoperative stage had been adamantinoma based on the patient's older age and aggressive imaging features, such as complete intramedullary involvement and perilesional marrow edema. However, both of those cases had intralesional fat in common. Therefore, we postulate that the presence of intralesional fat can be a clue to osteofibrous dysplasia rather than adamantinoma. Moderate to severe bone marrow or soft tissue edema is frequently associated with a pathologic fracture. Soft tissue edema was generally absent or mild without pathologic fracture.

Magnetic resonance images may assist in differentiating other tumors or tumor-like lesions which can simulate osteofibrous dysplasia in radiological features. Regarding small and unilocular osteofibrous dysplasia, osteoid osteoma, intracortical abscess and intracortical hemangioma should be included in the differential diagnosis. Compared with osteofibrous dysplasia, osteoid osteoma shows more extensive marrow and soft tissue edema with respect to the size of the nidus (29). An intracortical abscess displays peripheral rim enhancement compared with the diffuse enhancement pattern of osteofibrous dysplasia on contrast-enhanced MR images (30). Intracortical hemangioma

Korean Journal of Radiology
KJR

may contain lattice-like coarse trabeculations and fatty components (31). Regarding multilocular osteofibrous dysplasia, the differential diagnosis includes an aneurysmal bone cyst, osteoblastoma, intracortical fibrous dysplasia and adamantinoma. An aneurysmal bone cyst commonly exhibits fluid levels and marginal septal enhancement (32), while osteofibrous dysplasia displays diffuse enhancement. An osteoblastoma involving long bones frequently accompanies perilesional extensive marrow and soft tissue edema (33). Cortical-based fibrous dysplasia is not uncommon, particularly in the tibia (34). Fibrous dysplasia is known to have hyper- or hypointense signal in T2-weighted images depending on the components and exhibits a central or rim enhancement pattern (19). Adamantinoma has nearly the same signals as osteofibrous dysplasia in radiography. However, MR findings may provide additional information to distinguish both lesions as discussed above.

This study had several limitations. First, the MR parameters differed between cases, as the cases were retrospectively collected from different institutions. Thus, MR images of each case were inevitably obtained with different parameters from different MR scanners. Second, in most cases, fast spin-echo sequences were applied to obtain T2-weighted images. In conventional T2-weighted images, the signal intensity of fat is a good internal reference for discriminating between intermediate and high signal intensity of the tumor. However in T2-weighted images obtained by fast spin-echo, fat signal cannot be used as a reference of intermediate signal due to the fact that fat is much brighter in such than in conventional spin-echo techniques. Therefore, determining the signal intensity of lesions as intermediate or high signal based on fast spin-echo T2-weighted images may have been rather subjective. Finally, we cannot be certain that osteofibrous dysplasia-like adamantinoma was completely excluded in the present study. As discussed above, even pathologic examination cannot clearly discriminate between osteofibrous dysplasia and osteofibrous dysplasia-like adamantinoma, because both have nearly the same histologic components except for small foci of epithelial cells in osteofibrous dysplasia-like adamantinoma. However, considering this close resemblance in the histology of both lesions, our results would have been only minimally affected even if the osteofibrous dysplasia-like adamantinoma cases had been included.

In conclusion, osteofibrous dysplasia exhibited diverse imaging features ranging from lesions confined to the cortex to more aggressive lesions with complete intramedullary involvement or perilesional marrow edema. The knowledge of the variable MR findings of osteofibrous dysplasia may provide the basis for differentiating osteofibrous dysplasia from adamantinoma and other bone lesions simulating as osteofibrous dysplasia.

REFERENCES

1. Campanacci M, Laus M. Osteofibrous dysplasia of the tibia and fibula. *J Bone Joint Surg Am* 1981;63:367-375
2. Campbell CJ, Hawk T. A variant of fibrous dysplasia (osteofibrous dysplasia). *J Bone Joint Surg Am* 1982;64:231-236
3. Mirra JM, Picci P. *Osteofibrous dysplasia (juvenile adamantinoma?)*. In: Mirra JM, ed. *Bone Tumors-Clinical, Radiologic, and Pathologic Correlations*. Philadelphia: Lea & Febiger, 1989:1217-1231
4. Resnick D, Kyriakos M, Greenway GD. *Tumors and tumor-like lesions of bone: Imaging and pathology of specific lesions*. In: Resnick D, ed. *Diagnosis of Bone and Joint Disorders*, 4th ed. Philadelphia: Saunders, 2002:3796-3800
5. Goergen TG, Dickman PS, Resnick D, Saltzstein SL, O'Dell CW, Akeson WH. Long bone ossifying fibromas. *Cancer* 1977;39:2067-2072
6. Park YK, Unni KK, McLeod RA, Pritchard DJ. Osteofibrous dysplasia: clinicopathologic study of 80 cases. *Hum Pathol* 1993;24:1339-1347
7. Dominguez R, Saucedo J, Fenstermacher M. MRI findings in osteofibrous dysplasia. *Magn Reson Imaging* 1989;7:567-570
8. Khanna M, Delaney D, Tirabosco R, Saifuddin A. Osteofibrous dysplasia, osteofibrous dysplasia-like adamantinoma and adamantinoma: correlation of radiological imaging features with surgical histology and assessment of the use of radiology in contributing to needle biopsy diagnosis. *Skeletal Radiol* 2008;37:1077-1084
9. Gleason BC, Liegl-Atzwanger B, Kozakewich HP, Connolly S, Gebhardt MC, Fletcher JA, et al. Osteofibrous dysplasia and adamantinoma in children and adolescents: a clinicopathologic reappraisal. *Am J Surg Pathol* 2008;32:363-376
10. Springfield DS, Rosenberg AE, Mankin HJ, Mindell ER. Relationship between osteofibrous dysplasia and adamantinoma. *Clin Orthop Relat Res* 1994;(309):234-244
11. Murphey MD, wan Jaovisidha S, Temple HT, Gannon FH, Jelinek JS, Malawer MM. Telangiectatic osteosarcoma: radiologic-pathologic comparison. *Radiology* 2003;229:545-553
12. Goto T, Kojima T, Iijima T, Yokokura S, Kawano H, Yamamoto A, et al. Osteofibrous dysplasia of the ulna. *J Orthop Sci* 2001;6:608-611
13. Nakashima Y, Yamamuro T, Fujiwara Y, Kotoura Y, Mori E, Hamashima Y. Osteofibrous dysplasia (ossifying fibroma of long bones). A study of 12 cases. *Cancer* 1983;52:909-914

14. Williams HK, Mangham C, Speight PM. Juvenile ossifying fibroma. An analysis of eight cases and a comparison with other fibro-osseous lesions. *J Oral Pathol Med* 2000;29:13-18
15. Kahn LB. Adamantinoma, osteofibrous dysplasia and differentiated adamantinoma. *Skeletal Radiol* 2003;32:245-258
16. Teo HE, Peh WC, Akhilesh M, Tan SB, Ishida T. Congenital osteofibrous dysplasia associated with pseudoarthrosis of the tibia and fibula. *Skeletal Radiol* 2007;36 Suppl 1:S7-S14
17. Wang JW, Shih CH, Chen WJ. Osteofibrous dysplasia (ossifying fibroma of long bones). A report of four cases and review of the literature. *Clin Orthop Relat Res* 1992;(278):235-243
18. Jee WH, Choe BY, Kang HS, Suh KJ, Suh JS, Ryu KN, et al. Nonossifying fibroma: characteristics at MR imaging with pathologic correlation. *Radiology* 1998;209:197-202
19. Jee WH, Choi KH, Choe BY, Park JM, Shinn KS. Fibrous dysplasia: MR imaging characteristics with radiopathologic correlation. *AJR Am J Roentgenol* 1996;167:1523-1527
20. Utz JA, Kransdorf MJ, Jelinek JS, Moser RP Jr, Berrey BH. MR appearance of fibrous dysplasia. *J Comput Assist Tomogr* 1989;13:845-851
21. Van der Woude HJ, Hazelbag HM, Bloem JL, Taminiau AH, Hogendoorn PC. MRI of adamantinoma of long bones in correlation with histopathology. *AJR Am J Roentgenol* 2004;183:1737-1744
22. Ishida T, Iijima T, Kikuchi F, Kitagawa T, Tanida T, Imamura T, et al. A clinicopathological and immunohistochemical study of osteofibrous dysplasia, differentiated adamantinoma, and adamantinoma of long bones. *Skeletal Radiol* 1992;21:493-502
23. Markel SF. Ossifying fibroma of long bone: its distinction from fibrous dysplasia and its association with adamantinoma of long bone. *Am J Clin Pathol* 1978;69:91-97
24. Mori H, Yamamoto S, Hiramatsu K, Miura T, Moon NF. Adamantinoma of the tibia. Ultrastructural and immunohistochemic study with reference to histogenesis. *Clin Orthop Relat Res* 1984;(190):299-310
25. Sweet DE, Vinh TN, Devaney K. Cortical osteofibrous dysplasia of long bone and its relationship to adamantinoma. A clinicopathologic study of 30 cases. *Am J Surg Pathol* 1992;16:282-290
26. Bloem JL, van der Heul RO, Schuttevaer HM, Kuipers D. Fibrous dysplasia vs adamantinoma of the tibia: differentiation based on discriminant analysis of clinical and plain film findings. *AJR Am J Roentgenol* 1991;156:1017-1023
27. Czerniak B, Rojas-Corona RR, Dorfman HD. Morphologic diversity of long bone adamantinoma. The concept of differentiated (regressing) adamantinoma and its relationship to osteofibrous dysplasia. *Cancer* 1989;64:2319-2334
28. Hazelbag HM, Taminiau AH, Fleuren GJ, Hogendoorn PC. Adamantinoma of the long bones. A clinicopathological study of thirty-two patients with emphasis on histological subtype, precursor lesion, and biological behavior. *J Bone Joint Surg Am* 1994;76:1482-1499
29. Kransdorf MJ, Stull MA, Gilkey FW, Moser RP Jr. Osteoid osteoma. *Radiographics* 1991;11:671-696
30. Tehranzadeh J, Wong E, Wang F, Sadighpour M. Imaging of osteomyelitis in the mature skeleton. *Radiol Clin North Am* 2001;39:223-250
31. López-Barea F, Hardisson D, Rodríguez-Peralto JL, Sánchez-Herrera S, Lamas M. Intracortical hemangioma of bone. Report of two cases and review of the literature. *J Bone Joint Surg Am* 1998;80:1673-1678
32. Mahnken AH, Nolte-Ernsting CC, Wildberger JE, Heussen N, Adam G, Wirtz DC, et al. Aneurysmal bone cyst: value of MR imaging and conventional radiography. *Eur Radiol* 2003;13:1118-1124
33. Kroon HM, Schurmans J. Osteoblastoma: clinical and radiologic findings in 98 new cases. *Radiology* 1990;175:783-790
34. Lädermann A, Stern R, Ceroni D, De Coulon G, Taylor S, Kaelin A. Unusual radiologic presentation of monostotic fibrous dysplasia. *Orthopedics* 2008;31:282